# Parasitic Patch of the Same Dimensions Enabled Excellent Performance of Microstrip Antenna Array

**Mingchun Tang, Shaoqiu Xiao, Tianwei Deng, Duo Wang, and Bingzhong Wang**

The Institute of Applied Physics
University of Electronic Science and Technology of China, Chengdu, China, 610054
xiaoshaoqiu@uestc.edu.cn

***Abstract*** **-** This paper presents a thorough investigation on the use of parasitic patch as an effective secondary radiator to suppress mutual coupling and improve the gain of a microstrip array. The measured results show that the proposed parasitic patch placed halfway between elements in the *E*-plane of two-element array not only suppresses mutual coupling by 7.3dB, but, also, improves the gain by 1.6dB. By further simulation and comparison, the results indicate the proposed parasitic patch is quite suitable for application into the high-density microstrip arrays.

***Index Terms*** **-** Gain improvement, microstrip array, mutual coupling reduction, parasitic patch.

## I. INTRODUCTION

Microstrip arrays are used extensively due to their many attractive features, including low profile, light weight, and convenience for integrating with microwave monolithic integrated circuit (MMIC) technologies. Despite the above important advantages over other conventional antennas, there are some drawbacks which have prevented practical applications. One of the most severe problems is that, when the substrate with high dielectric constant is selected, the strong mutual coupling is accordingly incurred in virtue of the pronounced surface wave excitation [1-3]. To suppress unwanted surface wave, lots of methods are presented, such as loading electromagnetic band-gap (EBG) structures [4], mu-negative (MNG) metamaterials [5, 6], and defected ground structures (DGSs) [7]. However, they take on some inherent defects in applications. EBG needs complicated and high-cost design, and takes too much spacing; MNG metamaterials are of narrowband and little mechanical robustness; DGSs lead to inevitable strong backward radiation through the notched ground.

In this paper, the parasitic antenna of the same dimensions is proposed, and it is etched halfway between the two *E*-coupled microstrip antennas as a simple and effective way to suppress surface wave and improve the whole gain, due to its "secondary radiation" property.

## II. USING PARASITIC PATCH TO SUPPRESS MUTUAL COUPLING AND IMPROVE GAIN OF THE WHOLE ARRAY

The comprehensive studies related to the mutual coupling between adjacent microstrip antennas exist [8]. In a standard array configuration with a high permittivity substrate, the surface waves dominate and the coupling between elements in the *E*-plane orientation is greater than that in the *H*-plane [7]. Therefore, mutual coupling suppression between the *E*-plane-coupled elements is only investigated to validate the performance of the proposed parasitic antenna in Fig. 1. The parasitic antenna has the same dimensions of the two active antennas, and it is loaded halfway in the traditional probe-fed microstrip array, with the interelement spacing approximately three quarters of wavelength in free space.

The antenna arrays presented in this paper are all simulated using Ansoft HFSS [9], an electromagnetic simulator based on finite element method (FEM). Together with simulated results, the experimentally measured results of the array in Fig. 1 are entirely shown in Figs. 2 and 3. Because of strong surface waves, the mutual coupling ($S_{21}$) of -13.9dB in traditional array at the center resonant frequency 6.06GHz is observed in Fig. 2(a), which is in good agreement with the aforementioned analysis in Section I. When the parasitic patch of the same dimensions is etched halfway between the two elements as a secondary radiator in the *E*-plane, the mutual coupling drops to -21.2dB (7.3dB reduction) at the center

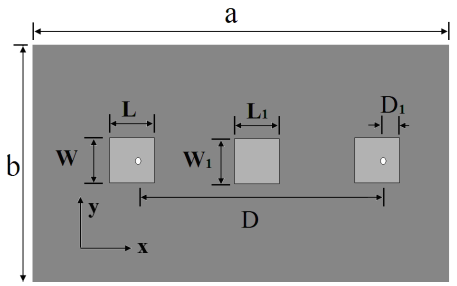


(a)

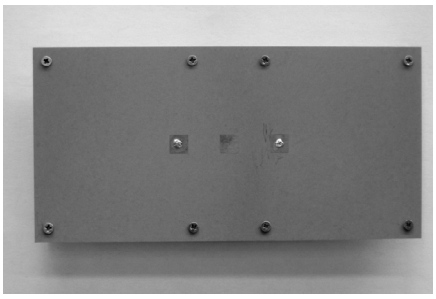

(b)

Fig. 1. Geometry of a two-element array with parasitic patch; the patches: $L= L_1=6.6mm$, $W=W_1=6.7mm$, the distance of the two active patches: $D=36mm$, the two probe-fed positions: $D_1$=4.2mm, the substrate ($a\times b=140mm\times 70mm$) with the dielectric constant $\varepsilon_r$=10.2 has the height = $2mm$. (a) dimensions in details, (b) fabricated antenna array.

resonant frequency 6.09 GHz in Fig. 2 (b). It is noticed that, due to the additional intercoupling between the active elements and parasitic element, there is a slight drift of the center resonant frequency occurrence (0.03GHz shifting).

The far-field radiation performance is also experimentally measured and compared as shown in Fig. 3. The side lobe drops distinctly and the gain pattern becomes smooth with no apparent ripples in comparison with that of the reference array [7], especially in the *E*-plane. As a secondary radiator, a certain surface wave constrained within substrate is radiated into front free space, which improves the whole array peak gain of radiation pattern in the front from 7.9dBi to 9.5dBi.

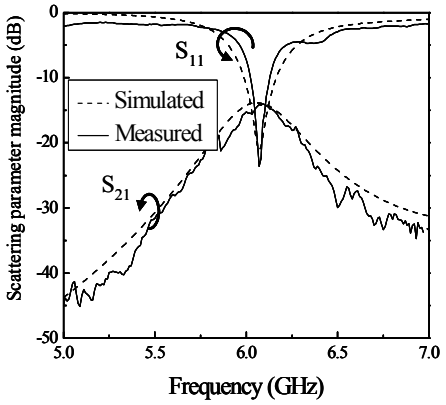


(a)

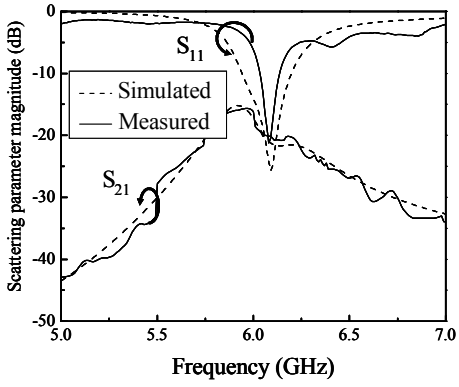


(b)

Fig. 2. Simulated and measured scattering parameters of the traditional array and parasitic patch loaded array. (a) traditional array, (b) parasitic patch loaded array.

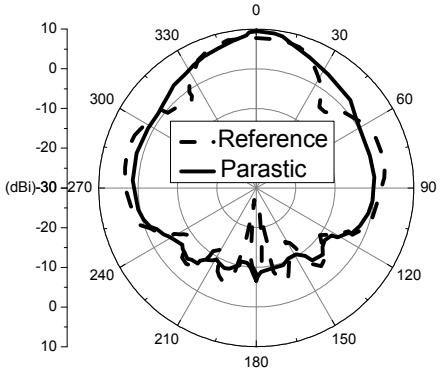


(a)

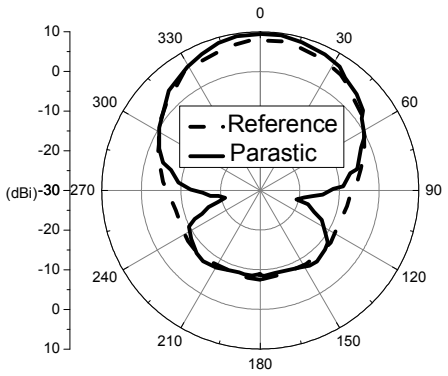


(b)

Fig. 3. Experimentally measured gain patterns of the traditional array and parasitic patch loaded array. (a) *E*-plane, (b) *H*-plane.

## III. RESULTS AND ANALYSIS

To analyze the electromagnetic characteristics of parasitic patch, the surface current distribution on the upper surface of the three identical patches at the center resonant frequency 6.09GHz is, also, simulated, and the sketch is drawn in Fig. 4. It is shown that when the two *E*-coupled antennas are excited with the same phases and magnitudes, the current on parasitic patch is synchronously induced, which is regularly polarized on the surface in accordance with that on the active patches. Certain EM energy could radiate through the parasitic patch and much more energy is guided upwards into free space by comparing traditional array and the array with parasitic patch as shown in Fig. 5. It is in good agreement with the measured results in Fig. 3, which improves the main lobe gain. In details, the near-field illumination created by the proposed parasitic-patch-loaded array is more uniform than the traditional two-element array, and it has cosine-shaped illumination amplitude shown in

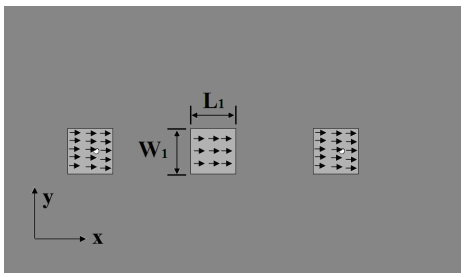


Fig. 4. Surface current distribution on all patches at resonance frequency.

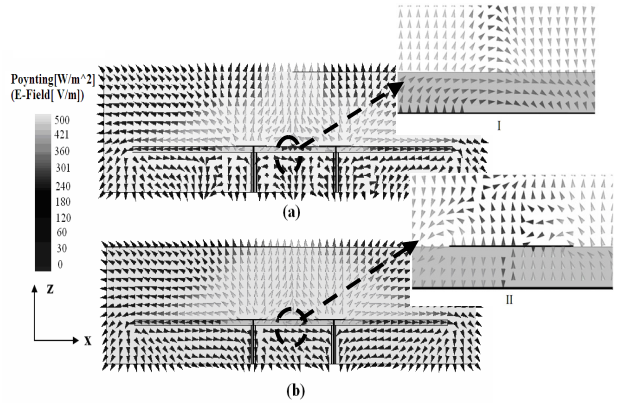


Fig. 5. Simulated Poynting vector distribution in *E*-plane of the two-element array and corresponding amplified *E*-field distribution images (I and II) in the middle places. (a) traditional array, (b) the array with parasitic patch.

Fig. 5(b), in opposition to the illumination in Fig. 5(a), which clearly shows some peaks in the Poynting vector amplitude. Therefore, the radiation diagram of the proposed parasitic-patch-loaded array has higher directivity (due to the fact that more uniform illumination creates a larger effective radiating aperture) and lower sidelobe level (as the cosine tapered amplitude illumination reduces diffraction at the edges of the patch), as it can be seen in the E-plane gain patterns shown in Fig. 3(a).

Furthermore, the current on the parasitic patch (in Fig. 4) is induced by surface wave in the substrate. It could be verified by comparing two amplified images in Fig. 5. The *E*-field of surface wave in the amplified image I is weak and homogeneous in the substrate. On the contrary, when the parasitic patch is loaded halfway, the *E*-field in the amplified image II is much stronger in the substrate. Besides, the *E*-field on the two sides of the parasitic patch is polarized in opposite phase, which demonstrates that the surface wave gives rise to parasitic patch resonance as two other active patches (Fig. 4). Accordingly, the parasitic patch acts as an energy director, and it guides the majority of the surface wave energy from the substrate into the front space so that the surface wave in the substrate degrades sharply. The reduction of surface wave interaction between the two active elements consequently incurs mutual coupling suppression (Fig. 2). Moreover, we add another probe-fed under the parasitic patch to excite it with the same phase. The simulation result demonstrates that the peak gain reaches 8.67dBi (which is lower than the array with

parasitic patch in Fig. 1), and the mutual coupling between two elements at the edges is -15.7dB (slight mutual coupling reduction 1.8dB). It is seen that the active patch exhibits much poorer performance in comparison with the parasitic one.

It can be seen that the parasitic patch has two functions: mutual coupling suppression and gain improvement. In contrast of the aforementioned inherent defects (methods of EBG, mu-negative metamaterials, and DGS loading), this method, conquering the above problems, exhibits particular properties when the elements in array are placed in high density.

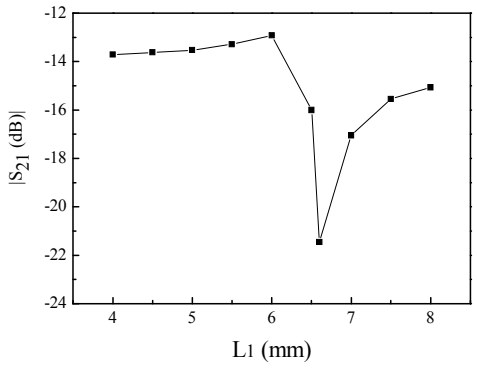


Fig. 6. The mutual coupling coefficient ($S_{21}$) against the length of parasitic patch $L_1$.

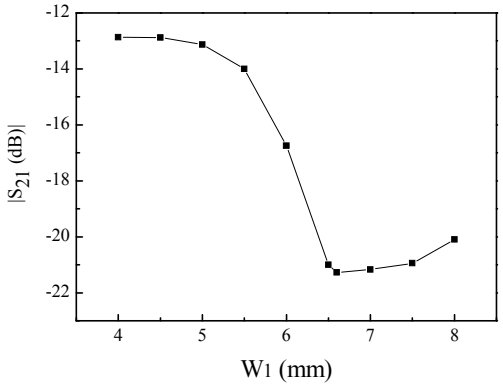


Fig. 7. The mutual coupling coefficient ($S_{21}$) against the width of parasitic patch $W_1$.

The dimensions of the parasitic patch are thoroughly simulated and compared in Figs. 6 and 7. Figure 6 gives the relationship between the mutual coupling $S_{21}$ and the length of the parasitic patch when the width is fixed to *6.7mm*. The results indicate when its length changes, the mutual coupling changes accordingly. Especially when $L_1=L=6.6mm$ is chosen, the best mutual coupling suppression ($S_{21}$= -21.3dB) is attained. Similarly, the mutual coupling, also, alters with variation of the parasitic patch width, and $W_1=W=6.7mm$ is the most suitable value for mutual coupling reduction, on the premise of the fixed length *6.6mm*, shown in Fig. 7. It can be seen that the parasitic patch can be utilized as a radiating patch operating at 6.09GHz. However, the best choice is the use of ordinary parasitic patch of the same dimensions as the radiating elements.

Moreover, the performance of the parasitic patch in mutual coupling suppression is further analyzed in Fig. 8. In order to validate its predominant capability, the results of traditional array are also listed in Fig. 8. When the elements are high-density placed in the *E*-plane with the variation of interelement distance between $0.5\lambda_0$ and $\lambda_0$ (where $\lambda_0$ is the wavelength in free space at the operation frequency), the mutual coupling

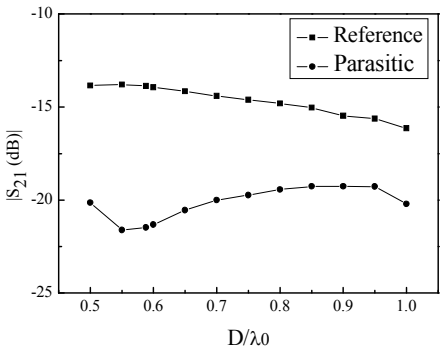


Fig. 8. The mutual coupling coefficient ($S_{21}$) against distance between two active elements in *E*-plane.

drops markedly (5-10dB), compared with the reference array. Thus, it is quite suitable to be utilized in a high density microstrip array application.

## IV. CONCLUSIONS

A simple and effective method to suppress mutual coupling is presented in this paper. The arrays with and without parasitic patch are measured and compared, respectively. The results demonstrate that the compact parasitic patch can suppress mutual coupling by 7.3dB, and improve the gain of the array by 1.6dB in a two-element

array. With the assistance of simulation analysis, the proposed parasitic patch with the same dimensions as the active elements is quite available to apply into high density microstrip array to suppress mutual coupling and improve the whole array radiation performance. In addition, due to low mutual coupling performance and simple configuration of the proposed parasitic patch, it can be a candidate for conformal phased array applications.

## ACKNOWLEDGMENT

This work was supported partially by the Hi-Tech Research and Development Program of China (Grant No. 2009AA01Z231), partially by the National Natural Science Foundation of China (Grant No. 60872034), and partially by the National Defense Pre-Research Foundation of China (Grant No. 08DZ0229, 09DZ0204).

## REFERENCES

[1] A. H. Mohammadian, Noel M. Martin, and Donald W. Griffin, "A theoretical and experimental study of mutual coupling in microstrip antenna arrays," *IEEE Trans. Antennas Propag.*, vol. 37, pp. 1217–1223, 1989.

[2] C. M. Krowne, "Dielectric and width effect on H-plane and E-plane coupling between rectangular microstrip antennas," *IEEE Trans. Antennas Propag.*, vol. 31, pp. 39–47, 1983.

[3] R. R. Ramirez and F. De Flaviis, "A mutual coupling study of linear and circular polarized microstrip antennas for diversity wireless systems," *IEEE Trans. Antennas Propag.*, vol. 51, pp. 238–248, 2003.

[4] N. Jin, A. Yu, and X. X. Zhang, "An enhanced 2×2 antenna array based on dumbbell EBG structure," *Microwave Opt.Technol. Lett.*, vol. 39, pp. 395–399, 2003.

[5] K. Buell, H. Mosallaei, and K. Sarabandi, "Metamaterial insulator enabled superdirective array," *IEEE Trans. Antennas Propag.*, vol. 55, pp.1074–1085, 2007.

[6] B.-L. Wu, H. Chen, J. Au Kong, and T. M. Grzegorczyk, "Surface wave suppression in antenna systems using magnetic metamaterial," *J. Appl. Phys.*, vol. 101, 2007.

[7] D.-B. Hou, S. Xiao, B.-Z. Wang, L. Jiang, J. Wang, and W. Hong, "Elimination of scan blindness with compact defected ground structures in microstrip phased array," *IET Microw. Antennas Propag.*, vol. 3, pp. 269-275, 2009.

[8] J. J. Pérez and J. A. Encinar, "A simple model applied to the analysis of E-plane and H-plane mutual coupling between microstrip antennas," *Proc. IEEE AP-S Int. Symp.*, vol. 1, pp. 520-523, 1993.

[9] Ansoft High Frequency Structure Simulation (HFSS), ver. 10, Ansoft Corp., 2005.